

# A High-Precision Strain-Measurement Bridge Circuit System with On-line Digital Calibration

Masashi Kono    Tetsuya Taura    Takahide Suzuki    Hiroshi Sunaga  
 Yoshihisa Yamada    Keigo Kimura    Masanao Morimura†    Haruki Okano††  
 Masami Iwazaki††    Hiroyuki Takuno††    Mitsumasa Suzuki††    Yukio Shinoda††  
 Haruo Kobayashi

Electronic Engineering Department, Gunma University  
 † Consultant    †† Tokyo Sokki Kenkyujo Co., Ltd.,

**Abstract**– This paper describes high-precision dynamic strain measurement bridge circuits with on-line calibration of parasitic capacitance effects. The proposed calibration system is very reliable and robust against temperature change because most of the calibration is done in digital domain.

**Keyword:** Strain Measurement, Strain Gauge, Bridge Circuit, Calibration.

## I. Introduction

Recently much attention is being paid to sensor technology for automotive applications. In this paper we focus on high-precision strain measurement technology (Figs.1, 2 and 3, [1]-[9]) for such applications. Strain measurement methods can be classified into DC (Fig.4) and AC (Fig.5) methods. DC methods are simple, but suffer from low-frequency noise (such as 50Hz or 60Hz hum noise from power supply), drift, and thermal electromotive force (emf), and hence cannot achieve high precision. On the other hand, while AC methods are not affected by low-frequency noise, drift, and thermal emf, they suffer from parasitic capacitance effects [1]. In this paper, we describe how we have attempted to solve this problem of parasitic capacitance effects, which have been a problem for a long time in AC methods of strain measurement, using ADC and modern digital technology.

## II. Principle of Strain Measurement with Strain Gauge and Bridge Circuit

When a material is stretched (or compressed), the force used generates a corresponding stress  $\sigma$  inside

the material. This stress in turn generates a proportional tensile strain (or compressive strain) which deforms the material by  $L + \Delta L$  (or  $L - \Delta L$ ), where  $L$  is the original length of the material. When this occurs, the strain is the ratio of  $\Delta L$  to  $L$  (Fig.1).

$$\varepsilon = \frac{\Delta L}{L}.$$

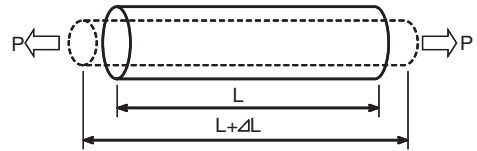


Fig. 1: Explanation of “Strain”.

Fig.2 shows an example of a strain gauge and a Wheatstone bridge circuit; there are several types of their combinations according to applications. Suppose that  $V_{in} = 2[V]$  is applied, and further suppose that the applied strain changes the gauge resistance from  $R$  to  $R + \Delta R$ .

Then the Wheatstone bridge circuit output voltage  $\Delta V$  is given by

$$\Delta V = \frac{\Delta R}{2R + \Delta R} = \frac{\frac{\Delta R}{R}}{2R + \frac{\Delta R}{R}} [V],$$

and we can obtain the strain value  $\varepsilon$  as

$$\varepsilon = \frac{2}{k} * \frac{\Delta V}{1 - \Delta V} \varepsilon \simeq \Delta V$$

where  $\Delta V = \frac{k\varepsilon}{2 + k\varepsilon} [V].$

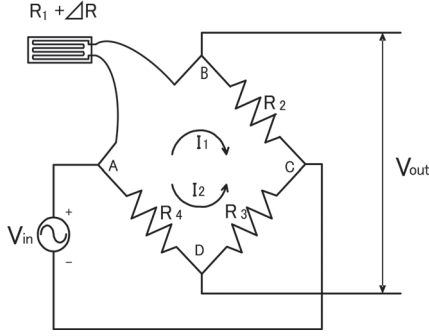


Fig. 2: Strain gauge and Wheatstone bridge circuit (quarter bridge 2-wire system).

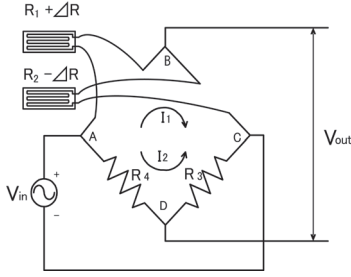


Fig. 3: Strain gauges and Wheatstone bridge circuit (half bridge system with 2-active method).

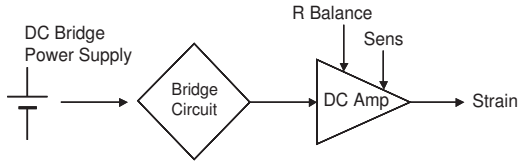


Fig. 4: DC-type dynamic strain measurement system.

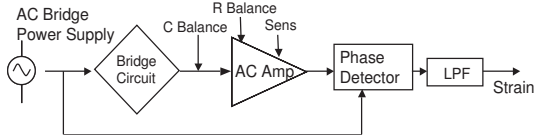


Fig. 5: AC-type dynamic strain measurement system.

### III. Analysis of Parasitic Capacitance Influences

In applications where the strain gauge must be at some distance from the strain measuring instrument, and so long wires must be used to connect them, the parasitic capacitance associated with the wires limits the accuracy of the measurement. In this section we analyze the parasitic capacitance effects. Fig.6 shows a bridge circuit with parasitic capacitances, and its transfer function  $H(j\omega)$  is given by :

$$H(j\omega) = \frac{Z_2 - Z_1}{Z_1 + Z_2}$$

$$Z_1 = \frac{R_1}{1 + j\omega C_1 R_1}$$

$$Z_2 = \frac{R_2}{1 + j\omega C_2 R_2}$$

The transfer function  $H(j\omega)$  can be rewritten as

$$H(j\omega) = \frac{H_N(j\omega)}{H_D(j\omega)}$$

$$H_N = R_2^2 - R_1^2 + \omega^2 R_1^2 R_2^2 (C_1^2 - C_2^2)$$

$$+ 2j\omega R_1 R_2 (R_1 C_1 - R_2 C_2),$$

$$H_D = (R_2 + R_1)^2 + \omega^2 R_1^2 R_2^2 (C_1 + C_2)^2.$$

We have checked the above equations by SPICE simulation in Fig.6 where simulation conditions are  $R_1 = 350 \Omega$ ,  $R_2 = 353 \Omega$ ,  $C_1 = 4000pF$ ,  $C_2 = 3500pF$ ,  $f = 20kHz$ ,  $V_{in} = 2V$  (Fig.7).

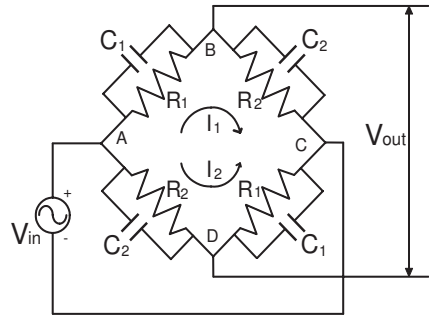


Fig. 6: A simplified model of a half bridge circuit with parasitic capacitances.

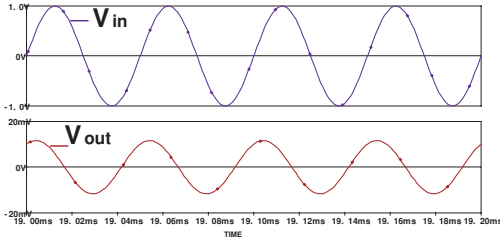


Fig. 7: SPICE simulation of input and output waveforms in the bridge circuit with parasitic capacitances in Fig.6.

Letting  $\varepsilon$  be the strain value (to be measured),  $k$  be the gauge ratio (a given value),  $\sigma$  be the poisson ratio (a given value), then resistor values  $R_1, R_2$  in the above equation for are replaced as follows

$R_1 \rightarrow R_1(1 + k\varepsilon)$ ,  $R_2 \rightarrow R_2(1 - L\varepsilon)$ ,  $L = k\sigma$ . Then  $H(j\omega)$  can be rewritten as  $H(j\omega) = H_R(j\omega) + jH_I(j\omega)$  where

$$\begin{aligned}
 H_R(j\omega) &= R_2^2(1 + k\varepsilon\sigma)^2 - R_1^2(1 + k\varepsilon)^2 \\
 &+ \omega^2 R_1^2 R_2^2 \\
 &(1 + k\sigma)^2(1 + k\varepsilon\sigma)^2(C_1^2 - C_2^2) \\
 &+ 2j\omega^2 R_1 R_2(1 + k\varepsilon)(1 - k\sigma\varepsilon) \\
 &\{R_1 C_1(1 + k\varepsilon) - R_2 C_2(1 - k\varepsilon\sigma)\}, \\
 H_I(j\omega) &= \{R_2(1 - k\varepsilon\sigma) + R_1(1 + k\varepsilon)\}^2 \\
 &+ \omega^2 R_1^2 R_2^2 \\
 &(1 + k\varepsilon)^2(1 - k\varepsilon\sigma)^2(C_1 + C_2)^2.
 \end{aligned}$$

We see that both the real and imaginary parts of  $H(j\omega)$  are affected by parasitic capacitances  $C_1, C_2$  (Fig.8) and they are also functions of  $\varepsilon$ ,  $\varepsilon^2$  and  $\varepsilon^3$ .

#### IV. Conventional Strain Measurement Method and its Problem

Conventional AC dynamic strain measurement systems measure the real part  $H_R(j\omega)$  of the bridge output voltage by phase detection and calculate the strain, assuming that  $C_1, C_2$  are small enough to be neglected, and also that  $\varepsilon$  squared and  $\varepsilon$  cubed can be neglected. However, in recent applications where parasitic capacitances are not negligible due to long wires from gauges to a bridge

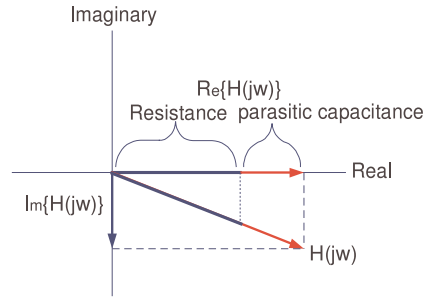


Fig. 8: Effect of parasitic capacitance effects on the real part of  $H(j\omega)$ .

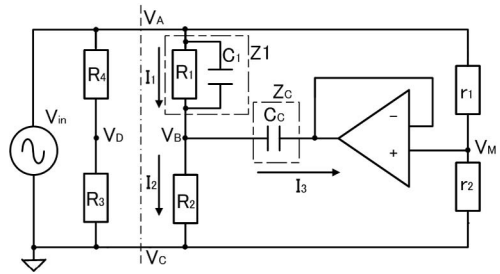


Fig. 9: An analog method for parasitic capacitances  $C_1$  compensation.

circuit and very high precision measurement is demanded, these assumptions are not valid any more. Sometimes an analog calibration method is used to compensate for parasitic capacitances as shown in Fig.9 (see Appendix), but due to temperature change and aging effects this method cannot satisfy more demanding requirements.

### V. Proposed Parasitic Capacitance Cancellation System

#### A. Configuration

Fig.10 shows our proposed strain measurement system, which has the following features:

- Oscillators of two different frequencies ( $\omega_1, \omega_2$ ) are used. ( $\omega_1/2\pi, \omega_2/2\pi$ ) are on the order of 10kHz.
- The bridge output is amplified by an AC amplifier which does not suffer from low frequency noise.
- The input and output signals of the bridge circuit are converted to digital data (with accuracy of 16 bits or greater) by delta-sigma modulators, and are

stored in memory.

(d) A digital signal processor compensates for parasitic capacitance and calculates  $\varepsilon$  taking into account  $\varepsilon^2$ ,  $\varepsilon^3$  effects.

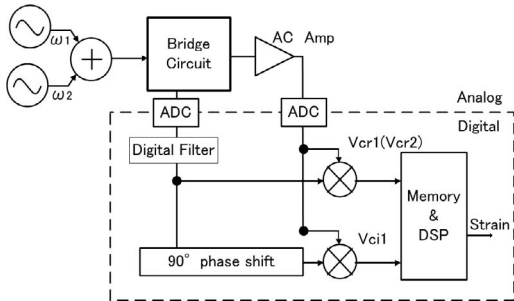


Fig. 10: Proposed dynamic strain measurement system.

## B. Algorithm

Our strain calculation algorithm is as follows:

(1) The input  $\cos(\omega_1 t) + \cos(\omega_2 t)$  is applied to the bridge circuit, and its input and output are converted to digital signals. Digital filter operation is performed to them so that the component of  $\cos(\omega_1 t)$  is extracted from the input part and also  $\omega_1$  component is obtained from the output. By multiplying the input  $\cos(\omega_1 t)$  and output  $\omega_1$  component signal, and taking the time average of the multiplication result in the digital domain, we have the value of  $H_R(j\omega_1) = V_{cr1}$ .

In other words, if the output  $\omega_1$  component signal  $V_{out1}(t) = a_1 \cos(\omega_1 t) + b_1 \sin(\omega_1 t)$ ,

$$\begin{aligned} \cos(\omega_1 t) \times V_{out}(t) &= \frac{a_1}{2} + \frac{a_1}{2} \cos(2\omega_1 t) \\ &+ \frac{b_1}{2} \sin(2\omega_1 t), \\ \text{then } H_R(j\omega_1) &= \frac{a_1}{2} = V_{cr1}. \end{aligned}$$

$$V_{cr1} = \frac{R_2^2(1 - k\varepsilon\sigma)^2 - R_1^2(1 + k\varepsilon)^2 + \omega_1^2 R_1^2 R_2^2(1 + k\sigma)^2(1 - k\varepsilon\sigma)^2(C_1^2 - C_2^2)}{\{R_2(1 - k\varepsilon\sigma) + R_1(1 + k\varepsilon)\}^2 + \omega_1^2 R_1^2 R_2^2(1 + k\varepsilon)^2(1 - k\varepsilon\sigma)^2(C_1 + C_2)^2} \quad (1)$$

$$V_{cr2} = \frac{R_2^2(1 - k\varepsilon\sigma)^2 - R_1^2(1 + k\varepsilon)^2 + \omega_2^2 R_1^2 R_2^2(1 + k\sigma)^2(1 - k\varepsilon\sigma)^2(C_1^2 - C_2^2)}{\{R_2(1 - k\varepsilon\sigma) + R_1(1 + k\varepsilon)\}^2 + \omega_2^2 R_1^2 R_2^2(1 + k\varepsilon)^2(1 - k\varepsilon\sigma)^2(C_1 + C_2)^2} \quad (2)$$

$$V_{ci} = \frac{2\omega_1^2 R_1 R_2(1 + k\varepsilon)(1 - k\sigma\varepsilon)\{R_1 C_1(1 + k\varepsilon) - R_2 C_2(1 - k\varepsilon\sigma)\}}{\{R_2(1 - k\varepsilon\sigma) + R_1(1 + k\varepsilon)\}^2 + \omega_1^2 R_1^2 R_2^2(1 + k\varepsilon)^2(1 - k\varepsilon\sigma)^2(C_1 + C_2)^2} \quad (3)$$

(2) In the same way, the input  $\cos(\omega_1 t) + \cos(\omega_2 t)$  is applied to the bridge circuit, and its input and output are converted to digital signals. Digital filter operation is performed to them so that the component of  $\cos(\omega_1 t)$  is extracted from the input part and also  $\omega_1$  component is obtained from the output. The input  $\cos(\omega_1 t)$  is phase-shifted by 90 degrees in the digital domain, to obtain  $\sin(\omega_1 t)$  precisely (Accurate 90-degree phase-shift in digital domain is one of advantages of our proposed system.) Then by multiplying  $\sin(\omega_1 t)$  and the output  $\omega_1$  component, and taking the time average of the multiplication result in the digital domain, we have the value of  $H_I(j\omega_1) = V_{ci}$ .

$$\begin{aligned} \sin(\omega_1 t) \times V_{out}(t) &= \frac{b_1}{2} - \frac{b_1}{2} \cos(2\omega_1 t) \\ &+ \frac{a_1}{2} \sin(2\omega_1 t), \\ \text{then } H_I(j\omega_1) &= \frac{b_1}{2} = V_{ci}. \end{aligned}$$

(3) Next we consider  $\omega_2$  component. The input  $\cos(\omega_1 t) + \cos(\omega_2 t)$  is applied to the bridge circuit, and its input and output are converted to digital signals. Digital filter operation is performed to them so that the component of  $\cos(\omega_2 t)$  is extracted from the input part and also  $\omega_2$  component is obtained from the output. By multiplying the input and the output, and taking the time average of the multiplication result in the digital domain, we have the value of  $H_R(j\omega_2) = V_{cr2}$ .

(4) Then we have the following three equations. Since the number of unknown parameters ( $\varepsilon, C_1, C_2$ ) is three and there are three equations, this problem can be solved. (Equation (1),(2),(3)).

**Remark** Digital domain calculation enables taking care of  $\varepsilon^2$ ,  $\varepsilon^3$  terms, which can realize more precise calculation than analog method.

## VI. Advantages of our Digital Method

Parasitic capacitance values are unknown and can change according to temperature and aging. Analog signal processing circuits may generate additional noises inside them. However the above-mentioned system and algorithm are digital, and they can reliably compensate for parasitic capacitance on-line. Delta-sigma ADCs with greater than 16bit accuracy and a few tens kilo Hertz bandwidth are now commercially available, and which, together with recent rapid progress of DSP, enable realization of our proposed system at low cost.

## VII. Evaluation of Proposed Algorithm Using Field Data

We have evaluated the proposed algorithm using the actual field data for one gauge system (Fig.2).

(i) We have applied a sinusoidal input of 5kHz (or 20kHz) to the bridge circuit with parasitic capacitances of 1,000pF (or 2,000pF, 3,000pF), and the bridge circuit output is fed to the following AC amplifier.

(ii) We have collected AD-converted input data to the bridge circuit, and AD-converted output data of the AC amplifier using a strain measurement instrument. Note that we do not have to implement hardware of digital processing parts for its evaluation, and calculation by software is enough for that purpose.

(iii) We have estimated the amplitudes and phases of the actual input and output sine waves using a sine curve fitting algorithm (Fig.11) which we have developed with C program [10], and obtained the real imaginary part values of the transfer function.

(iv) We have calculated the strain and the parasitic capacitance values using the obtained values and the proposed algorithm.

(v) We have also calculated the strain value using the conventional algorithm (which uses only the real part and ignores the parasitic capacitance).

(vi) We have compared the results calculated by the proposed and conventional algorithms, and confirmed the precision of the proposed algorithm.

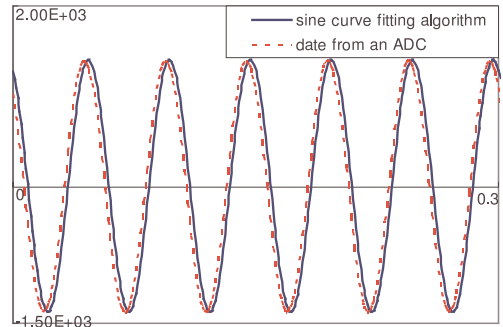


Fig. 11: A dotted line shows field data of sinusoidal signal as ADC output, and a solid-line indicates an estimated sine curve using the curve fitting algorithm.

Fig.12 shows the calculation results using field data. X-axis indicates the parasitic capacitance value, and Y-axis shows an error from the true strain value ( $10,000\mu\varepsilon$ ). We see that the proposed algorithm reduces the error from 1.4 % to 0.5 % with parasitic capacitance value of 3,000pF and input frequency of 5kHz, and from 49 % to 3.4 % with parasitic capacitance value of 3,000pF and input frequency of 20kHz.

## VIII. Conclusions

We have proposed a high-precision strain measurement system based on modern ADC and digital technology. In recent applications strain gauges have to be put on objects under strain measurement far from strain measurement instruments, which require long lines with associated parasitic capacitances; in such cases parasitic capacitances degrade measurement accuracy significantly and cause drift. The proposed algorithm can cancel them on-line in digital domain, which is reliable and accurate. We have demonstrated its effectiveness by simulation and experiment using field data.

**Acknowledgement** We would like to thank Prof. H. Yamasaki, Mr. I. Tazawa and Mr. K. Wilkinson for valuable comments.

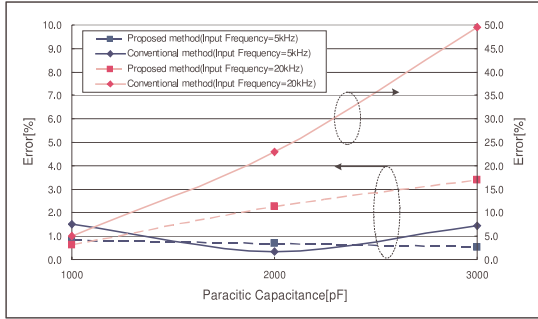


Fig. 12: Accuracy comparison of strain measurement between proposed and conventional algorithms using field data.

## References

- [1] H. Sunaga, M. Kono, T. Taura, K. Kimura, M. Morimura, H. Okano, M. Iwasaki, H. Takuno, M. Suzuki, H. Kobayashi, "High-Precision Strain Measurement Bridge Circuit With Calibration of Parasitic Capacitance Effects", Technical Meeting on Electronic Circuits, IEEJ, ECT-06-28, Kiryu (March. 2006).
- [2] T. Taura, M. Kono, H. Sunaga, K. Kimura, M. Morimura, H. Okano, M. Iwasaki, H. Takuno, M. Suzuki, H. Kobayashi, "High-Precision Strain Measurement Bridge Circuit System", The 23th Sensing Forum, The Society of Instrument and Control Engineers, (Oct. 2006).
- [3] M. Kono, T. Taura, H. Sunaga, K. Kimura, T. Suzuki, M. Morimura, H. Okano, M. Iwasaki, H. Takuno, M. Suzuki, H. Kobayashi, "A High-Precision AC Wheatstone Bridge Strain Gauge", 2006 IEEJ International Analog VLSI Workshop, Hangzhou, China (Nov. 2006).
- [4] J. J. Carr, Elements of Electronic Instrumentation and Measurement, Third Edition, Prentice Hall (1996).
- [5] McGraw-Hill Concise Encyclopedia of Science and Technology, McGrawHill (1998).
- [6] B. Liptak, Instrument Engineer's Handbook, Process Measurement and Analysis CRC Press LLC (1995).
- [7] Analog Devices Inc. Op Amp Applications, CQ Publishing (2003).
- [8] Omegadyne Pressure, Force, Load, Torque Data-book, Omegadyne Inc. (1996).
- [9] Strain Gauge Users' Guide, Tokyo Sokki Kenkyujo Co. Ltd.

- [10] Y. Motoki, H. Sugawara, H. Kobayashi, T. Komuro, and H. Sakayori, "Multi-Tone Curve Fitting Algorithms for Communication Application ADC Testing," Electronics and Communication in Japan: Part II: Electronics, Wiley Periodicals Inc. vol.86, no.8, pp.1-11 (2003).

## Appendix

This appendix describes a conventional analog method to compensate parasitic capacitances  $C_1$  (Fig.7).  $C_1$  effects are compensated when the ratio of  $r_1$  to  $r_2$  is adjusted so that the current  $I_c$  which flows through  $C_1$  is equal to  $I_3$ , and then  $I_2$  and the current which flows through  $R_1$  are equal. (In other words, parasitic capacitance  $C_1$  is compensated by  $C_c, r_1, r_2$  and the operational amplifier). Currents  $I_1, I_2, I_3$  and voltages  $V_D, V_M$  are given by

$$\begin{aligned}
 I_1 &= I_2 + I_3, \\
 I_1 &= \frac{V_{in} - V_B}{Z_1}, \quad I_2 = \frac{V_B}{R_2}, \\
 I_3 &= \frac{V_B - V_M}{Z_c}, \quad V_M = \frac{r_2}{r_1 + r_2} V_{in}. \\
 V_B &= \frac{R_2 + j\omega R_1 R_2 (C_1 + \alpha C_c)}{R_1 + R_2 + j\omega R_1 R_2 (C_1 + C_c)} V_{in}. \\
 (\because Z_1 &= \frac{R_1}{1 + j\omega R_1 C_1}, \quad Z_c = \frac{1}{j\omega C_c}).
 \end{aligned}$$

Hence, the current  $I_c$  which flows  $C_1$  is given by

$$I_c = \frac{R_1 + j\omega R_1 R_2 C_c (1 - \alpha)}{R_1 + R_2 + j\omega R_1 R_2 (C_1 + C_c)} j\omega C_1 V_{in}.$$

Also  $I_3$  is can be rewritten as

$$I_3 = \frac{-\alpha R_1 - R_2 (1 - \alpha) + j\omega R_1 R_2 C_c (1 - \alpha)}{R_1 + R_2 + j\omega R_1 R_2 (C_1 + C_c)} \times j\omega C_2 V_{in}.$$

Here,  $\alpha = r_2 / (r_1 + r_2)$ . Then we can derive that the condition for  $I_c = I_3$  is

$$\frac{r_2}{r_1} = \frac{C_c R_c - C_1 R_1}{R_1 (C_c + C_1)}.$$

With this condition, the parasitic capacitance  $C_1$  effects are compensated. However, the value of  $C_1$  may be unknown and also it may change according to temperature and aging, and furthermore automatic adjustment of the ratio  $r_2/r_1$  is difficult; thus its complete cancellation with this analog method is very difficult.